Understanding Eastern Himalayan Cryosphere Using Remote Sensing

by

Saurabh Kaushik

10PP18J15003

A thesis submitted to the
Academy of Scientific & Innovative Research
for the award of the degree of
DOCTOR OF PHILOSOPHY
in
(SCIENCE)

Under the supervision of

Dr. Tejpal Singh and **Prof. P.K. Joshi**

CSIR-Central Scientific Instruments Organisation, Chandigarh

Academy of Scientific and Innovative Research
AcSIR Headquarters, CSIR-HRDC campus
Sector 19, Kamla Nehru Nagar,
Ghaziabad, U.P. – 201002, India

January
2023

CERTIFICATE

This is to certify that the work incorporated in this Ph.D. thesis entitled, 'Understanding Eastern Himalayan Cryosphere Using Remote Sensing", submitted by Saurabh Kaushik to the Academy of Scientific and Innovative Research (AcSIR) in fulfillment of the requirements for the award of the Degree of DOCTOR OF PHILOSOPHY in SCIENCE, embodies original research work carried-out by the student. We, further certify that this work has not been submitted to any other University or Institution in part or full for the award of any degree or diploma. Research material(s) obtained from other source(s) and used in this research work has/have been duly acknowledged in the thesis. Image(s), illustration(s), Figure(s), table(s) etc., used in the thesis from other source(s), have also been duly cited and acknowledged.

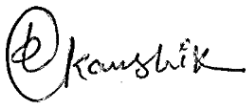

(Signature of Student)
Name: Saurabh Kaushik
Date: 13/02/2023

(Signature of Co-Supervisor)
Name: Prof. P.K. Joshi
Date: 13/02/2023

(Signature of Supervisor)
Name: Dr. Tejpal Singh
Date: 13/02/2023

STATEMENTS OF ACADEMIC INTEGRITY

I, Saurabh Kaushik, a Ph.D. student of the Academy of Scientific and Innovative Research (AcSIR) with Registration No. 10PP18J15003 hereby undertake that the thesis entitled "Understanding Eastern Himalayan Cryosphere Using Remote Sensing" has been prepared by me and that the document reports original work carried out by me and is free of any plagiarism in compliance with the UGC Regulations on "*Promotion of Academic Integrity and Prevention of Plagiarism in Higher Educational Institutions (2018)*" and the CSIR Guidelines for "*Ethics in Research and in Governance (2020)*".

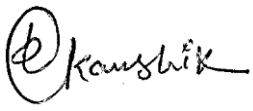

Signature of the Student
Date : 13/02/2023
Place : Chandigarh

It is hereby certified that the work done by the student, under my/our supervision, is plagiarism-free in accordance with the UGC Regulations on "*Promotion of Academic Integrity and Prevention of Plagiarism in Higher Educational Institutions (2018)*" and the CSIR Guidelines for "*Ethics in Research and in Governance (2020)*".

Signature of the Co-supervisor
Name : Prof. P.K. Joshi
Date : 13/02/2023
Place : New Delhi

Signature of the Supervisor
Name : Dr. Tejpal Singh
Date : 13/02/2023
Place : Chandigarh

ACKNOWLEDGEMENTS

Writing a PhD is considerably more than just the process of writing a manuscript, the last five years have been a remarkable experience. I am thankful to so many people who have been a source of consistent support, inspiration and help over the last five years. Big thanks to my two supervisors, Dr. Tejpal Singh and Prof. P.K. Joshi for keeping me motivated throughout my PhD duration, and sending me all over the world for conferences, training and exchange programs. Prof. P.K. Joshi and Dr. Tejpal Singh have always pushed me to bring the best out of me and walked me through all sorts of technical and institutional challenges. I am highly thankful to my supervisors for their unconditional support and foster my scientific career beyond my expectations.

I am grateful to Director CSIR-CISO, AcSIR-CSIO coordinator (Prof. Vinod Karar and Prof. Sanjeev Soni) and Head of Department (Mr. Amitava Das) for consistent support, motivation, and all the required infrastructural facilities. I extend my gratitude to Mr. Suneet Sapra, assistant manager AcSIR-CSIO for his consistent support in smoothly inducting every AcSIR formality. I am also highly thankful to the entire Team of 'Polar and Cold region' (Prof. Claudia, Dr. Andreas Dietz, Dr. Celia Baumhoer, Dr. Mariel Dirscherl, Jonas Köhler; Marius Philipp, Dr. Sebastian Rößler at Germany Aerospace Center (DLR), where I spent 18 months as an exchange Ph.D. student. The incredible working experience at DLR has resulted in some of the best work carried out throughout my PhD duration. Danke schön!

This doctoral work would not have been possible without the support of various institutions which provided valuable funds and promoted me to excel without hardship. I would acknowledge the funding support from Innovation in Science Pursuit for Inspired Research (INSPIRE) GoI. I acknowledge the support received from Deutscher Akademischer Austauschdienst (DAAD) for granting the bi-nationally supervised doctoral research grant that funded my travel and stay in Germany for a period of 18 months. The equipment support received from the Sustainable Natural Resource Use in Arctic and High Mountainous Areas (SUNRAISE) and Urban Resilience and Adaptation for India and Mongolia (URGENT) projects, co-funded by the Erasmus+ Programme of the European Union has helped in efficiently completing the laboratory work, thus are duly acknowledged. I would also like to thank the National Aeronautics and Space Administration (NASA), Japan Aerospace Exploration Agency (JAXA) and European Space Agency (ESA) for the free of cost data provided by them to carry out my research work.

Special thanks to all my colleagues and friends (Nitin Mohan Sharma, Vikas Kumar, Vikas Shaw, Dr. Lalit Maurya, Neha, Parul, Priyanka, Tarandeep Singh, Dr. Yogesh

Kumar, Raman Kaushal, Lavlesh, Vishavpreet Singh, and Vipasha Sharma) at CSIR-CSIO who have always been there for productive discussion over tea breaks, extended lunches, and dinners. I also owe thanks to my friends (Ram, Deepanshu, Pankaj, KK, Neeraj, Arvind, Ganjendra, Chinu, Divanshu and Vishal) for filling all these years with all sorts of adventure and fun. The unforgettable trips and time with all helped me to go through all the stressful times.

Lastly not the least I wish to thank my family: their support has always been a driving force for pursuance of excellence. My parents (Mr. Subhash Chand and Mrs. Raj Rani) unconditionally supported me throughout my career and held every decision of mine. My siblings (Dr. Jitendra Kaushik, Mr. Gaurav Sharma and Mrs. Madhuri) always took care of my financial and emotional support, things won't be the same and smooth without their support. Above all, all these won't be possible without the blessings of 'Lord Shiva'.

Saurabh Kaushik

Table of Contents

CERTIFICATE ii
STATEMENTS OF ACADEMIC INTEGRITY iii
ACKNOWLEDGEMENTS iv
Table of Content vi
List of Figure x
List of Table xv
Abbreviations xvi

Chapter 1 1
1. Introduction 1
1.1. Background 1
1.2 Relevance of Himalayan Cryosphere 4
1.2.1. Physiographic relevance 4
1.2.2. *Socio-economic relevance* 7
1.3 State of Himalayan Cryosphere 8
1.4 Research Motivation 9
1.5 Research gaps and Objectives 10
1.6 Structure of Thesis 11

Chapter 2 13
2. A review of Himalayan cryosphere with especial emphasis on Eastern Himalaya 13
2.1. Glacier Mapping 14
2.1.1. Rationale of the glacier mapping 14
2.1.3. Remote Sensing of glacier extent 19
2.1.4. Mapping of debris cover glacier 27
2.1.5. Existing approaches and emerging area of research 40
2.1.6. Errors associated with glacier mapping 42
2.1.7. Recommendations 43
2.2. Glacier Velocity 43
2.3. State of glacial lake mapping 47

Chapter 3 51
3. A methodological framework for automated Supraglacial-debris extraction 51
3.1. Deep learning for glacier mapping 52
3.2. Input Data 53
3.2.1. Sentinel 1data 55
3.2.2. Sentinel 2 data 55
3.2.3. Landsat 8 data 55
3.2.4. ALOS DEM 56
3.2.5. Training labels 56
3.2.6. Training and testing sites 57
3.3. Methodology 58
3.3.1. Pre-Processing and Data Preparation 58
3.3.2. Deep Neural Network Architecture (SGDNet) 60
3.3.3. Post Processing 62
3.3.4. Accuracy Assessment 62
3.4. Results 64
3.4.1. Proposed Deep Artificial Neural Network (SGDNet) 64
3.4.2. Test Site 1, 2, and 3 66
3.4.3. Generating glacier dataset for Sikkim Himalaya 70
3.5. Discussion 74
3.5.1. Testing different band combinations 74
3.5.2. Classification Results and Comparison with Existing Methods 77
3.5.3. Limitations and Future Work 80
3.5.4. Summary 81

Chapter 4 82
4. A methodological framework for automated glacial lake extraction 82
4.1. Deep learning for glacial lake mapping 83
4.2. Input Data 84
4.2.1. Training labels 85
4.2.2. Training and testing sites 86
4.3. Methodology 87
4.3.1. Pre-Processing and Data Preparation 88
4.3.2. Deep Convolutional Neural Network Architecture (GLNet) 89

4.3.3. Post Processing 92
4.3.4. Accuracy Assessment 93
4.3.5. GLOF hazard assessment 94
4.4. Results 96
4.4.1. Proposed Deep Convolutional Artificial Neural Network (GLNet) 97
4.4.2. Classification results for test sites (1, 2, 3 and 4) 97
4.4.2. Generating glacier dataset for Sikkim Himalaya 102
4.5. Discussion 105
4.5.1. Testing different band combinations 106
4.5.2. Methodological advances and comparison with existing methods 108
4.5.3. Methodological limitations and future requirement 113
4.5.4. Summary 115

Chapter 5 117
5. Spatio-temporal glacier surface velocity estimation using time series satellite data 117
5.1. Glacier surface velocity estimation 117
5.2. Input Data 118
5.2.1. Landsat Data 118
5.2.2. SRTM DEM 119
5.2.3. Study site 120
5.3. Methodology 122
5.3.1. Glacier velocity and topographic control estimation 122
5.3.2. Uncertainty estimation 125
5.4. Results 126
5.4.1. Spatiotemporal variation in glacier velocity 127
5.4.2. Impact of glacier size and debris cover on velocity 130
5.4.3. Impact of slope on glaciers velocity 132
5.5. Discussion 135
5.5.1. Understanding spatiotemporal variability in glacier velocity 135
5.5.2. Comparison with other studies 138
5.5.4. Summary 142

Chapter 6 143
6. Synthesis and outlook 143

6.1. Summary and conclusive findings 143
6.2. Future outlook 146

References 150

Appendix 166

List of Publications 186

List of Figures

Figure 1.1 Cryosphere's component and their timescale; adapted from IPCC – AR4 WGI Chapter 4: Observations: Changes in Snow, Ice, and Frozen Ground. 2
Figure 1.2 The Electromagnetic Spectrum: The remote sensing sensor are designed to sense the specific range of EMR (usually varies from visible (0.4mm) to microwave (1m)). Credit: miniphysics.com..... 3
Figure 1.3 The extent of the Himalaya and Karakoram, major relevance is shown. The boundaries are taken from Bolch et al., (2012). The MODIS and SRTM DEM is used as base map..... 6
Figure 2.1 Overview of glacier mapping studies in Himalaya..... 16
Figure 2.2 Reflectance spectra of different snow and ice surfaces (Hall and Martinec 1985). 26
Figure 2.3 (a) Generalized cross-section of a typical valley glacier showing glacier boundary as a boundary between supraglacial and periglacial debris, Figure courtesy of (Shukla et al., 2010) (b) Shows the spectral similarity between supraglacial debris (SGD) and periglacial debris (PGD). VRK, valley rock; MID, mixed ice and debris..... 26
Figure 2.4 Results of some semi-automated approach for debris cover delineation using a combination of multiple dataset. (a) Debris cover glacier boundary delineated via semiautomated algorithms using multispectral imagery and DEM derived parameter (Paul, Huggel, and Andreas 2004), (b) Debris cover glacier boundary delineated using synergistic approach (Shukla et al., 2010), (c) Glacier boundary extracted using hybrid CNN+ Radom Forest (RF) approach (Nijhawan, Das, and Balasubramanian 2018), (d) Overlay of glacier boundary delineated using combination of optical and thermal data over high resolution satellite imagery (Karimi et al. 2012), (e) glacier boundary obtained via semi-automated approach, utilizing input from optical, thermal and surface curvature (Bhardwaj et al. 2014). This Figure illustrates, most of the studies demonstrated a semi-automated approach for debris cover delineation on very small geographical area (i.e. 1or two glaciers) which reduces the involved complexity of glacial terrain..... 33
Figure 2.5 (A) Map of some significant glacier velocity studies carried out in the Himalaya and Karakoram. This map does not include study reported by Dehceq et al. (2019) which provides a regional assessment of glacier velocity concentrated only on large (>5 km^2) glaciers. Yellow box shows location of study area, (ISM - Indian Summer Monsoon). Inset map shows location of Himalaya and Karakoram on world map. The boundary of the Himalayan region is taken from Bolch et al. (2012). 44
Figure 3.1 Spatial distribution of the test (blue) and training (red) sites across the Himalaya and Karakoram regions. The star denotes region, which was used as both training and testing data. The Himalayan and Karakoram boundaries were taken from Nie et al. (2017). 57
Figure 3.2 Deep learning neural network (DNN) architecture used for delineation of supraglacial debris (SGDNet). The numbers indicate the total number of unit (i.e., neurons) in each layer. The input layer consists of 9 bands (B: blue, G: green, R: red, NIR: near-infrared, SWIR: shortwave infrared, T: thermal, C: coherence, S: slope, and E: elevation). The output of the developed DNN is D: debris or ND: non-debris..... 61

Figure 3.3 Workflow for automated supraglacial debris mapping using remote sensing and deep learning. 63
Figure 3.4 Loss and accuracy curve of proposed DNN architecture (SGDNet) for SGD classification. 65
Figure 3.5 Supraglacial debris mapping in Sikkim, Eastern Himalaya using the proposed algorithm. False-positives and false-negatives were mapped manually using reference data. Red, white, green, and yellow boxes provide a contextual overview of the Figure 3.14A, 3.14B, 3.14C, and 3.14D. 66
Figure 3.6 Supraglacial debris mapping at test site 1 (Northwest Karakoram) using the proposed algorithm. False-positives and false-negatives were mapped manually using reference data 67
Figure 3.7 Supraglacial debris mapping at test site 2 (Karakoram) using the proposed algorithm. False-positives and false-negatives are mapped manually using reference data.. 68
Figure 3.8 Supraglacial debris mapping at test site 3 (Karakoram) using the proposed algorithm. False-positives and false-negatives are mapped manually using reference data. The red box provides a contextual overview of Figure 3.13. 69
Figure 3.9 Compiled glacier dataset of Sikkim Himalaya. 70
Figure 3.10 Comparison of glacier boundaries mapped in the present study with the available glacier inventories. The glacier boundary delineated in the present study also overlaid on google earth image for visual comparison. 72
Figure 3.11 Comparison of glacier boundaries mapped in the present study with the available glacier inventories. The glacier boundary delineated in the present study also overlaid on google earth image for visual comparison. 73
Figure 3.12 The loss and accuracy curve of proposed DNN for SGD classification using a combination of remote-sensing data. A - Optical-SAR-TIR-S; blue, green, red, NIR, SWIR, coherence, and slope, B - Optical-TIR-S-E; blue, green, red, NIR, SWIR, and slope, C - Optical-SAR-TIR; blue, green, red, NIR, SWIR, SAR, and TIR. 75
Figure 3.13 Qualitative analysis of results obtained using different combinations of bands. A - Optical-SAR-TIR-S-E (blue, green, red, NIR, SWIR, coherence, slope, and elevation), B - Optical-SAR-TIR-S (blue, green, red, NIR, SWIR, coherence, and slope), C - Optical-TIR-S-E (blue, green, red, NIR, SWIR, and slope), D - Optical-SAR-TIR (blue, green, red, NIR, SWIR, SAR, and TIR). The classification results obtained from the Optical-SAR-TIR-S-E layer showed better dis-crimination of SGD from PGS. The contextual information of Figure is presented in Figure 3.8. 77
Figure 3.14 Visual comparison of the results derived by the proposed algorithm with the available reference data. RGI-corrected data show a corrected glacier boundary on ~2015 satellite data by Herreid and Pellicciotti (2020). The RGI updated shows the minor corrections to Herreid and Pellicciotti (2020) glacier boundary as per scene characteristics. Supraglacial debris data exhibit the supraglacial debris extent by Herreid and Pellicciotti (2020), and DNN-derived shows the results of the proposed algorithm. The contextual information of Figure 3.14 A, B, C, and D is presented in Figure 3.5. 79
Figure 4.1 Location map of chosen training (red) and test (yellow) sites across the Himalaya. The inset map exhibits the location of the Himalayan and Karakoram. The glacier lake

boundaries are taken from Chen et al. (2021). The Karakoram and Himalayan boundaries were adopted from Nie et al. (2017). 86
Figure 4.2 Overview of the proposed GLNet. The inputs to the architecture are 10 pre-processed bands (i.e., B, G, R, NIR, SWIR, TIR, SAR coherence, slope, elevation, and NDWI). The features of the input image are an extracted series of convolution layers (encoder) and a fully connected layer (decoder) providing the final output. 90
Figure 4.3 The overall workflow of the proposed scheme. 92
Figure 4.4 Pairwise comparison matrix of factors affecting Glacial Lake Outburst Flood (GLOF). 95
Figure 4.5 Pairwise comparison matrix of factors affecting Glacial Lake Outburst Flood (GLOF). 95
Figure 4.6 Glacial Lake mapping over test site 1, Eastern Himalaya using the proposed GLNet. The GLNet derived lake boundaries are compared with the reference data to estimate error of commission (FP) and omission (FN). The red and yellow rectangles show a location of lakes displayed in the Figure 4.14 and Figure 4.15. 98
Figure 4.7 Glacial Lake mapping over test site 2, Eastern Himalaya using the proposed GLNet. The GLNet derived lake boundaries are compared with the reference data to estimate error of commission (FP) and omission (FN). The red rectangles show a location of lakes displayed in the Figure 4.14. 99
Figure 4.8 Glacial Lake mapping over test site 3, Eastern Himalaya using the proposed GLNet. The GLNet derived lake boundaries are compared with the reference data to estimate error of commission (false-positive) and omission (false-negative). The red rectangles show a location of lakes displayed in the Figure 4.14. 100
Figure 4.9 Glacial Lake mapping over test site 4, Eastern Himalaya using the proposed GLNet. The GLNet derived lake boundaries are compared with the reference data to estimate error of commission (false-positive) and omission (false-negative). The red rectangles show a location of lakes displayed in the Figure 4.14. 101
Figure 4.10 Glacial lake dataset generated over entire Sikkim Himalaya. The stream network is extracted via STRM 30m DEM using hydrological tools in ArcGIS. 103
Figure 4.11 Comparison of generated glacier lake dataset of Sikkim Himalaya with existing datasets (e.g., Chen et al., 2020 and Zhang et al., 2021). The comparison reveals supremacy of the dataset generated in the present study. 104
Figure 4.12 Glacial Lake Outburst Flood hazard assessment in Sikkim Himalaya. 105
Figure 4.13 The results of the proposed GLNet on all three-test site; (a) correlation analysis of GLNet derived lake boundaries and reference lake boundaries; (b) box plot showing size distribution of mapped glacial lakes via GLNet. 106
Figure 4.14 Example of precise glacial lake mapping via proposed GLNet across all three test sites. GLNet successfully mapped glacial lakes of varied appearance and size across all three test sites. T1; refers to test site 1, respectively T2; test site 2, T3; test site 3 and T4; test site 4. The location of these lakes are displayed in the Figure 4.6, 4.7, 4.8 and 4.9. 109
Figure 4.15 Visual comparison of most commonly used method for glacial lake mapping. A) represent the test site; B) represent result derived via NDWI thresholding method; C) exhibits automated glacial lake extraction using DNN (SGDNet(Kaushik et al., 2022b)); and D) shows

the results of the proposed method (GLNet) for glacial lake mapping. Contextual overview of Figure is provided in Figure 4. 110
Figure 4.16 Visual comparison between DeepLabV3+ and GLNet for glacial lake extraction. The GLNet outperformed DeepLabV3+, as DeepLabV3+ proved to be insignificant for classifying glacial lakes with varied lake turbidity (D and E). 112
Figure 4.17 Major limitations of GLNet; a, b, d represent an example of wet ice which is falsely predicted as lake over test site 1 and 2; (c) represent false prediction of shadow as glacial lake and (e) and (f) shows false negative prediction of frozen lakes over test site 2. 114
Figure 5.1 (B) Map of study area showing studied glaciers and topography. The glacier boundaries are taken from Randolph Glacier Inventory Version 6 (RGI V6) and Advanced Land Observing Satellite (ALOS) - Phased Array type L-band Synthetic Aperture Radar (PALSAR) (12.5 m) DEM is used for displaying topography. Fastest flowing glacier (ID 2, Zemu) and all other marked glaciers such as ID0 = South Lohnak, ID21 = Middle Lohnak, and ID22= North Lohnak, provide contextual information for Figure 5.6 and 4.7. The red and black box provides a contextual overview of Figure5.4 and 5.5. 121
Figure 5.2 Flow chart of overall methodology. 125
Figure 5.3 Trend in glacier velocity of Sikkim Himalaya. Linear trend, the deviance bar shows the estimated uncertainty in velocity for the particular image pair (A), Box plot showing heterogeneity in glacier velocity in the Sikkim Himalaya (B). The uncertainty associated with particular image pair is given in table 3. 127
Figure 5.4 Spatiotemporal variability in glacier velocity across Sikkim Himalaya. A) Glacier velocity estimated during 1994-1996 and B) Glacier velocity estimated during 2017-2018. Notice clear slowdown in the Zemu glacier. 128
Figure 5.5 Temporal snapshots of glacier slowdown in the Zemu glacier. A) velocity estimation during 1994-1996, b) velocity estimation during 2009-2010 and c) velocity estimation during 2017-2018. The glacier velocity is derived from image pairs of Landsat using COSI-Corr. Notice clear slowdown in up glacier. 129
Figure 5.6 Impact of glacier size and debris cover on glacier velocity in the Sikkim Himalaya during 1994-2020. A) Velocity variation among the different sizes of Glaciers. B) Velocity variation among different debris cover extent glaciers. DCG; Debris Cover Glacier (debris cover >25%), SDCG; Sparsely Debris Cover Glacier (debris cover >10 and <25%) and CIG; Clean Ice Glacier (debris cover < 10%). 131
Figure 5.7 Impact of slope on glacier velocity in the Sikkim Himalaya. (A) Relationship between slope and glacier velocity considering all glaciers. (B) Relationship between slope and glacier velocity for medium and large glaciers. 132
Figure 5.8 Computed Glacier velocity and surface slope along the central flow line for the selected glaciers (G0, G1, G2, G3, G18, G19, G21, G23 and G50) during (1994-2020). The glacier velocity and surface are resampled at every 120 m. 134
Figure 5.9 Comparison between glacier velocity estimated along central flowline and including all pixels for selected glaciers in the study region. Glacier velocity estimated along central flowline exhibits higher velocity signal. 140
Figure S.1Illustration of algorithm workflow and post-processing steps. A – results obtained via proposed Deep Neural Network (SGDNet), B – results obtained via first post-processing

step (if DNN result>0.3 and elevation>3300), C – cleaning up of result using 5×5 median filter and D – shows results after vectorization, the red polygons (<0.02) are removed from final results.....166
Figure S.2 Impact of shadow on classification accuracy of the proposed algorithm. A – presence of shadow in a satellite image, B – classification of shadow as false positive in the results obtained via proposed algorithm.....167
Figure S.3 Examples of generated label data. The generated label data comprised of glacial lakes of different size, shape and appearance. The special emphasis is laid on the inclusion of frozen and partly frozen lakes.....170
Figure S.4 Examples of generated label data. The generated label data comprised of glacial lakes of different size, shape and appearance. The special emphasis is laid on the inclusion of frozen and partly frozen lakes.....171
Figure S.5 Loss and accuracy curve of the proposed GLNet. 172
Figure S.6 Detailed analysis of proportion of wet ice and shadow in false positive area including all four test sites.....172
Figure S.7 Off glacier pixels consider for error estimation (2001-2002).....177
Figure S.8 Off glacier pixels consider for error estimation (2017-2018).....177
Figure S.9 Scatter plot of glacier size and average glacier velocity during 1994-2020. The larger glaciers correspond to higher glacier velocity. 178
Figure S.10 Glacier area distribution of the studied glaciers, 128 glaciers are having size <10 km^2 (Out of 133 glaciers).....178
Figure S.11 Four fastest flowing glaciated regions (red rectangles). All these regions are present in the clean ice zones with icefalls and crevasses. (Image Soure: Copernicus Sentinel 2; scene Id = L1C_T45RXL_A019221_20201110T044603. 179

List of Tables

Table 1.1 Glacier Inventory for Himalaya-Karakoram (HK) region compiled from various studies as referred in the text (Azam et al., 2019). 9
Table 2. 1 Overview of some significant studies shown in Figure 1.17
Table 2. 2 Summary of some significant glacier's studies carried out in the Indian Himalaya using manual digitization method. 21
Table 2. 3 Summary of some significant studies reported glacier delineation using supervised classification. 28
Table 2. 4 Overview of some significant glacier velocity studies shown in Figure 2.5. 45
Table 3.1 List of Sentinel 2 Spectral bands with central wavelength and resolution (Source Sentinel-2 user guides). 56
Table 3.2 Results of the proposed algorithm on the test sites. 69
Table 3.3 The comparison of the generated glacier dataset with available glacier inventories 71
Table 3.4. Results of the proposed deep artificial neural network (SGDNet) model using a combi-nation of optical, thermal, coherence, and slope as input layers. 74
Table 4.1 Results of the proposed GLNet on the chosen test sites. 101
Table 4.2 Comparison of glacial lake (area and number) reported in the present study with recently published datasets. 102
Table 4.3 A sensitivity analysis for different weighting schemes. 105
Table 5.1 List of Landsat satellite data used to estimate glacier velocity 119
Table 5.2 Estimated uncertainty in velocity for each Image pair and average for the entire period. 126
Table 5.3 Statistical results of Sikkim glacier velocity trend analysis (Mann-Kendall and Sen's slope). 134
Table S.1 Data used in the present study 167
Table S.2 Results of the various used Deep Artificial Neural Network models on the test data. 169
Table S.3 Lake characteristics of the chosen training data 173
Table S.4 Data used in the present study 174
Table S.5 SIV of individual glacier over the entire study period (1994-2020) 180

Abbreviations

ASTER	Advanced Spaceborne Thermal Emission and Reflection Radiometer
COSI-Corr	Co-registration of Optically Sensed Images and Correlation
CNN	Convolutional Neural Network
DEM	Digital Elevation Model
DCNN	Deep Convolutional Neural Network
DNN	Deep Neural Network
ELA	Equilibrium Line Altitude
ESA	European Space Agency
ETM+	Enhanced Thematic Mapper Plus
GIS	Geographic Information System
GLOF	Glacial Lake Outburst Flood
GLNet	Glacial Lake Net
GSI	Geological Survey of India
ICIMOD	International Centre for Integrated Mountain Development
InSAR	Interferometric Synthetic Aperture Radar
NASA	National Aeronautics and Space Administration
NCC	Normalized Cross Correlation
MSS	Multispectral Scanner
NDSI	Normalized Difference Snow Index
NDVI	Normalized Difference Vegetation Index
NIR	Near Infrared
NDWI	Normalized Difference Water Index
OLI	Operational Land Imager
PGD	Periglacial Debris
ReLU	Rectified Linear Unit
SAR	Synthetic Aperture Radar
SGD	Supraglacial Debris
SGDNet	Supraglacial Debris Net
SNR	Signal to Noise Ratio
SOI	Survey of India
SRTM	Shuttle Radar Topography Mission
SWIR	Shortwave Infrared
TM	Thematic Mapper
TSL	Transient Snowline

Co-funded by the
Erasmus+ Programme
of the European Union

Last Page

The appended material is based on research carried out at the partner institution of URGENT Project, and has potentially utilised the equipment support, inputs based on course revised/developed and training programs (*lecture series, research seminar and webinars*) through the URGENT Project.

The document is part of thesis part of PhD/MSc/MA research work carried out at the Jawaharlal Nehru University. Purposefully limited pages are shared to avoid copyright and other issues. However, the full thesis can be shared on request.

The complete thesis can be obtained from Prof P K Joshi (pkjoshi27@hotmail.com or pkjoshi@mail.jnu.ac.in).

Disclaimer: The European Commission's support for the production of this publication does not constitute an endorsement of the contents, which reflect the views only of the authors, and the Commission cannot be held responsible for any use which may be made of the information contained therein